British Journal of Applied Science & Technology
4(24): 3501-3518, 2014

SCIENCEDOMAIN
www.sciencedomain.org

Estimation of Evaporation from a Reservoir in Semi arid Environments Using Artificial Neural Network and Climate Based Models

Mostafa Ali Benzaghta[1*]

[1]*Soil and Water Department, Faculty of Agriculture, Sirte University, Libya.*

Author's contribution

This whole work was carried out by the author MAB.

Original Research Article

Received 4th March 2013
Accepted 1st September 2013
Published 30th June 2014

ABSTRACT

Estimation of evaporation from reservoirs in arid and semi-arid regions is a very crucial issue. This paper presents an application of Artificial Neural Networks (ANN) and climate based models (Penman, Priestley-Taylor and Stephens-Stewart), for the estimation of evaporation from the Algardabiya Reservoir, near Sirt, Libya. Daily meteorological data were collected for the years 2004 to 2006 and used to develop the evaporation estimation models. The measured meteorological variables included daily observations of air temperature, relative humidity, and wind speed. A statistical analysis was undertaken to verify the accuracy of the studied models. The results of the climate based and ANN models are compared with observed evaporation data from the reservoir. The comparison shows that there was better agreement between the ANN model estimations and the observed evaporation than the climate based models.

Keywords: Evaporation; artificial neural network; modeling; reservoir; Algardabiya Reservoir semi arid region.

1. INTRODUCTION

Water resource managers are confronted with the great challenge of scarcity. Scarcity is increasingly becoming the most important environmental constraint limiting plant growth in many regions. For example, over 30 arid and semi-arid countries are expected to have water

**Corresponding author: E-mail: benzaghta69@gmail.com;*

scarcity in 2025. This will consequently slow development, threaten food supplies, and aggravate rural poverty [1].

To respond to limitation of water and climate constraints (high temperature and low rainfall), Libya has constructed one of the greatest civil engineering groundwater pumping and conveyance systems which is called the Manmade River Project (MRP). This project was undertaken to supply Libya's water needs by drawing water from aquifers beneath the Sahara Desert and conveying it using a network of huge underground pipes (predominantly for irrigation) in Libya's northern coastal strip. The significant concern are the high cost of water pumping and the lack of appropriate planning system for efficient use of the water [2].

Evaporation is defined as the loss of stored water due to change from liquid state to vapor state, and it is affected by the climate condition such as temperature, wind speed, and solar radiation. For example, in hot and dry areas in Australia, it is estimated that about 95% of the rain evaporates and does not contribute to runoff. Water, when harvested, is commonly stored in storage reservoirs and dams, but it is estimated that up to half of this may be lost to evaporation [3]. The World Meteorological Organization (WMO) reported that three quarters of the total input (inflow and over-lake rainfall) to Lake Victoria in the U.S. is lost to evaporation, which results in relatively humid conditions [4]. In Egypt's Lake Nasser where the Nile's water is stored, downstream water loss due to evaporation is estimated to be 3 meters in depth, or double that of Lake Victoria. Lake Nasser is located in a very arid area that experiences hot desert climate.

Accurate estimation of evaporation loss from the water body is of primary importance for monitoring and allocating water resources. In hydrological practice, evaporation is directly measured by using an evaporation pan. The 'Class A' pan is one of the most widely used instruments for evaporation measurement and it has been used by many researchers around the world [5-9]. Analytically, mathematical models could be used to estimate evaporation from related meteorological variables like temperature, relative humidity, solar radiation, wind speed etc. Many researchers have developed models for estimating free water evaporation all over the world, [10,11,12,13,14]. These methods vary greatly in their ability to define the magnitude and variability of evaporation and require data that are not easily available.

Despite the large amount of published literature in this area, most of the reported methods are too demanding for observed meteorological data and prone to errors if locally calibrated parameters are not available [15]. In addition, evaporation is an incidental, nonlinear, complex, and unsteady process, so it is difficult to derive an accurate formula to represent all the physical processes involved. As a result, there is a new trend in using data mining techniques such as fuzzy logic, artificial neural networks (ANN) to estimate evaporation. ANNs have an advantage over deterministic models with respect to data needs which are less and well-suited for long-term forecasting [16].

The modeling experience in using ANN for evaporation estimation is still limited in comparison with a wider application in other fields such as flood forecasting, reservoir inflow forecasting, rainfall-runoff forecasting, and water quality forecasting [17,18,19,20,21]. There is a need to report results of application of this technique for regions with different climate conditions (semi-arid and humid regions) so that some generalization of this method could be achieved. Data from class A evaporation pan have been used for ANN model training and testing. The idea is to develop an accurate model for predicting evaporation from reservoirs

and to fill the missing evaporation data. Also, the model should be capable to predict past and future events using meteorological data.

The main objective of this study is to investigate the ability of the ANN technique to accurately estimate the daily evaporation from semi-arid environments using Algardabiya Reservoir in Libya as a case study. In this study meteorological and pan evaporation data were used to develop the ANN model and the output from this model was compared with the performance of selected climate based models.

1.1 Study Area Description

In this study, Algardabiya Reservoir was chosen as study reservoir in a semi-arid region. This reservoir (Sirte-Libya, 31º 09' 30.71" N; 16º 40' 58.02" E, 50 m.a.s.l) is a part of the Manmade River Project as shown in Fig. 1.

The reservoir is a earth embankment basin located 10 km south east of the City of Sirte, and adjacent to the coastal highway. The reservoir has a crest diameter of 887.66 m, and an operating depth of 12.5 m, giving it a maximum volume of 6.9 million cubic meters [22].

Fig. 1. The Location of the Algardibyia Reservoir in Sirte, Libya

1.2 Description of Data

Meteorological data for Algardibyia Reservoir area was acquired from the Meteorological Observatory of the Manmade River Authority, Sirte, Libya, and used to estimate evaporation. The meteorological data included maximum and minimum air temperature, relative humidity, wind speed, and class A evaporation pan records. The pan evaporation values were multiplied by a factor of 0.69 to estimate the actual evaporation from the Algardabiya Reservoir [23]. Three years of daily evaporation records from 2004 to 2006 were used to study the evaporation from Algardabiya Reservoir. Table 1 shows the various meteorological

Table 1. Descriptive Statistics of the Algardibyia Reservoir

Variables*	Units	Minimum	Maximum	Mean	SD	CV (SD/mean)
MaxTemp	°C	10	44	25.70	6.88	0.27
MinTemp	°C	4	32	14.97	5.57	0.37
AvTemp	°C	8.5	36	20.18	5.80	0.29
WS	Km/hr	5	50	14.63	7.78	0.53
RH	%	30	95	60.82	12.28	0.20
EVP	mm/d	3.7	15.2	7.66	2.29	0.30

* MaxTemp is maximum air temperature; MinTemp is minimum air temperature; AvTemp is average air temperature; WS wind speed; RH is relative humidity; EVP pan evaporation; CV is variation coefficient

2. ARTIFICIAL NEURAL NETWORKS MODEL (ANN)

The artificial neural network consists of nodes, also known as processing elements, which are distributed in the layers of the network by connections known as weights. All the processing nodes are arranged into layers, and each layer is fully interconnected to the following layer. There is no interconnection between the nodes of the same layer. In the model, there is an input layer that acts as a distribution structure for the meteorological data being presented to the network. After this layer, one processing layer follow, called the hidden layer. The final processing layer is called the evaporation layer. This type of ANN is called multilayer perceptron (MLP) [24]. Fig. 2 shows the structure of the ANN model, which is adopted in this study.

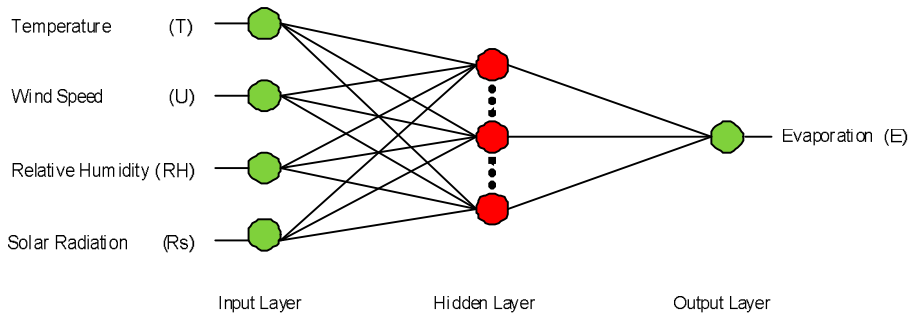

Fig. 2. Structure of ANN model

Each node in a layer receives and processes weighted input from a previous layer and transmits its output to nodes in the following layer through links. Each link is assigned a weight, which is a numerical estimate of the connection strength. The weighted summation of inputs to a node is converted to an output according to a transfer function (typically a sigmoid function). A feed forward neural network with back propagation (BPNN) training algorithm was selected for developing the ANN model because it is the most commonly used approach in hydrological modeling [25,26,27].

The feed forward back propagation neural network algorithm during the training process has two passes of propagation (forward/back propagation) for calculating all the gradients. For

the forward pass, the activation pattern of a meteorological variable is propagated through the network to produce an evaporation rate (output target). Each meteorological variable (x_j) is multiplied by an adjustable constant weight ($w_{i\,j}$) before being fed to the i^{th} processing element (PE) in the output layer.

In this study, the transfer function was the sigmoid which is one of the most commonly used transfer functions. This function takes the meteorological variables and squeezes the output into the range 0–1. The sigmoid activation function is defined as one of the most commonly used transfer function [24]. The sigmoid activation function for the continuous and differential process is defined for any meteorological variable, x as:

$$f(x) = \frac{e^x}{e^x + 1} \tag{1}$$

The function value approaches unity asymptotically as x gets larger, and $f(x)$ approaches zero asymptotically as x becomes negatively greater in value.

In the forward propagation, the computation of the evaporation rate is carried out, layer by layer, from the meteorological variables to the evaporation rate in the forward direction, and the error (ε) between predicted evaporation and observed evaporation is computed.

The data collected from the Algardabiya Reservoir was divided into two parts. Seventy per cent (70%) from 2004 to 2005 of the data was used for the purpose of training by minimizing the error data and the remaining thirty per cent (30%) of 2006 used for checking the overall performance of the trained network. In this study, the neural network was first fed with four inputs set and represented an ANN-1 model. ANN-2 model had three input variables and ANN-3 was designed as temperature-based model resenting similarity to the one of conventional methods selected in this study. The input variables combinations used to develop the ANN models are summarized in Table 2.

Table 2. Neural network input data structure.

Model	Inputs
ANN-1	Tempreture, Wind speed. Humidity and Solar Radiation
ANN-2	Tempreture, Wind speed and Humidity
ANN-3	Tempreture and Solar Radiation

2.1 Evaporation Models Descriptions

The following evaporation models have been chosen for this study because of their wide acceptance in the estimation of evaporation in many humid environments.

2.1.1 Penman model

Penman ([14,28]) presented theory and a method for the estimation of evaporation from meteorological data. He derived an equation to estimate evaporation from open water surfaces. The Penman equation is based on Dalton's law which has the following expression, ([29], c.f. [30]):

$$E = (e_s - e_a) f(u) \quad (2)$$

where:
E is the rate of evaporation in unit time; e_s is the saturation vapor pressure at the temperature of the water surface, (*kPa*); e_a is the vapor pressure in the air, (*kPa*) and $f(u)$ is a function of the wind speed u, (*m/sec*).

The Penman formula can be written as follows ([31]):

$$E_{PEN} = \frac{\Delta}{\Delta + \gamma} \times R_n + \frac{\gamma}{\Delta + \gamma} \times f(u)\, D \quad (3)$$

where:
E_{PEN} is open water–evaporation (*mm/d*); Δ is the slope of the saturation vapor pressure curve (*kPa/°C*); R_n is net radiation (*MJ/m²/d*); γ is psychrometric coefficient (*kPa/°C*); *f(u)* is wind function; D = (e_s-e_a) is vapor pressure deficit (*kPa*); e_s is saturation vapor pressure (*kPa*); e_a is actual vapor pressure (*kPa*).

In Penman's development, Equation (8), did not include heat exchange with the ground, or water advected energy, or change in heat storage. This assumption is acceptable for monthly or daily estimations in practical hydrological applications ([11,32-34]). The standardized calculation procedure for estimating the variables in Equation (8) from readily available data as recommended by Shuttleworth [34] and Allen et al. [32] are as follows:

$$\Delta = 4098\, e_s / (237.3 + T_a)^2 \quad (4)$$

$$\gamma = 0.00163 \frac{P}{\lambda} \quad (5)$$

$$R_n = R_s (1 - \alpha) \quad (6)$$

$$\lambda = 2.501 - T_a\, 2.361 \times 10^{-3} \quad (7)$$

$$f(u) = 2.62\, (1 + 0.536\, u_2) \quad (8)$$

$$e_a = 0.6108 \times \exp\left[\frac{17.27\, T_a}{T_a + 237.3}\right] \quad (9)$$

$$e_s = e_a / RH \quad (10)$$

where:
T_a (°C) is the average air temperature, P (*kPa*) is the air pressure; λ is the latent heat of vaporization (*MJ/kg*); R_s (*MJ/m²/d*) is the incoming solar radiation; α is the reflection coefficient or albedo constant (0.05) ([35]); u_2 (*m/s*) is the wind speed at 2 *m* height; and *RH* (%) is the relative humidity.

2.1.2 Priestley–Taylor model

Priestley and Taylor [36] proposed a simplified version of Penman's combination equation for use when surface areas are generally wet, which is a condition for evaporation. When the aerodynamic component is deleted and the energy component is multiplied by a coefficient

(β =1.26) with either wet or under humid conditions in the surrounding area and for large bodies of water, β was found to tend to 1.26 [37,38,39]. Therefore, it is possible to write the Priestley- Taylor Equation as follow:

$$E_{P-T} = \beta \left[\frac{\Delta}{\Delta + \gamma} \times \frac{R_n}{\lambda} \right] \tag{11}$$

where:

E_{P-T} is the open water-evaporation (*mm/d*); and β is the Priestley-Taylor coefficient. Other notations have the same meaning and units as in Equation (8).

2.1.3 Stephens and Stewart model

Stephens and Stewart [40] derived an Equation which requires only radiation and temperature data to estimate evaporation. This model is described as:

$$E_{S-S} = (a + b\,T_a)\,R_s \tag{12}$$

where:

E_{S-S} is the open water-evaporation (*mm/d*); T_a (ºC) is the average air temperature; R_s is the incoming solar radiation expressed as equivalent water evaporation (*mm/day*); *a* and *b* are fitting constants which are determined through least square method. Solar radiation, R_s, was calculated with the Angstrom formula [34,32].

2.1.4 Model performance

The performance of each model was studied by evaluating its statistical performance. To ensure a rigorous comparison of the models, an extended analysis was performed using different statistical indices for the estimated values. The three most widely used statistical indicators in estimation models are the coefficient of determination R^2, the root mean square error (*RMSE*) and the mean bias error (*MBE*) [41,42]. The above statistical indicators used are defined as:

$$R^2 = \frac{E_o - E}{E_o} \tag{13}$$

$$E_o = \sum_{i=1}^{n} \left(E_{i,obs} - E_{mean} \right)^2 \tag{14}$$

$$E = \sum_{i=1}^{n} \left(E_{i,obs} - E_{i,pred} \right)^2 \tag{15}$$

$$RMSE = \left[\frac{1}{n} \sum_{i=1}^{n} \left(E_{i,pred} - E_{i,obs} \right)^2 \right]^{1/2} \tag{16}$$

$$MBE = \frac{1}{n}\sum_{i=1}^{n}\left(E_{i,pred} - E_{i,obs}\right) \quad (17)$$

where:
$E_{i,obse}$ is the observed evaporation, mm/day, $E_{i,pred}$ is the predicted evaporation, mm/day, E_{mean} is the mean evaporation, and n is the number of data pairs.

3. RESULTS AND DISCUSSION

To assess the efficiency of the neural networks in predicting the evaporation losses from the Algardibyia Reservoir, a total of 731 data sets (2004 to 2005) were used in the present study for model building and validation. Also, a total of 365 data sets (2006) were used to test a model fitted to predict the evaporation. In this paper, ANN (i, j, k) indicates network architecture with i, j, and k neurons in the input, hidden, and output layers, respectively. In order to find the best ANN model alternative, the following parameter values are used: i from 2 to 4, j from 2–12, and k =1. The neural networks were trained with hidden nodes and after each training run, *MSE* and R^2 were calculated using only the training data set to find the optimal number of hidden nodes. The network architectures (4-6-1) for model ANN-1, (3-8-1) for model ANN-2 and (2-10-1) for model ANN-3 gave the minimum *MSE* of 0.094, 0.089 and 0.070 mm^2/d, respectively, and gave the highest coefficient of correlation for the standard back-propagation (Table 3). Thus, these three ANN architectures provided the best training results were applied to the test data.

Table 3. Neural network architectures and their statistic performance for the training data

Model	Network architecture	MSE	R^2
ANN-1	(4-6-1)	0.094	0.98
ANN-2	(3-8-1)	0.089	0.99
ANN-3	(2-10-1)	0.07	0.99

Daily meteorological data for the year 2006 (testing data set) were used to estimate evaporation from the selected climate based models (Penman model, Priestly and Taylor model, Stephens and Stewart model) and the ANN models. The comparison and evaluation of the climate based evaporation model and the ANN model with observed evaporation values from the Algardabiya Reservoir as the reference were made.

The performance of each model was tested by evaluating its statistical performance. To ensure a rigorous comparison of the models, an extended analysis was performed using *RMSE*, *MBE* and R^2 as statistical indices for the estimated values. Fox ([41]) and Willmott ([42]) pointed out that commonly used correlation measures, such as (R) and (R^2) in the testing of statistical significance in general are often inaccurate or misleading when used to compare model predicted and observed variables. The two most widely used statistical indicators in estimation models are the Root Mean Square Error (*RMSE*) and the Mean Bias Error (*MBE*) [42,43].

The *RMSE* is said to provide information on the short-term performance of a model by allowing a term-by-term comparison of the actual difference between the observed value and the predicted ones. The smaller the value, the better is the model's performance [42]. A drawback of this test is that few large errors in the sum can produce a significant increase in

RMSE. Furthermore, the *MBE* is said to provide information on the long-term performance of a model. A positive value gives the average amount of over-estimation in the estimated values and *vice versa*. The smaller the absolute value, the better is the model performance [42]. It is obvious that the *RMSE* and *MBE* statistical indicators, if not used in combination with one another, may not be an adequate indicators of a model's performance.

The statistical performance of climate based models and ANN models during test period are given in Table 4. It indicated that the ANN models were found to have lower *RMSE* and absolute *MBE* values and higher R^2 compared to climate based models. Therefore, the ANN models perform was better than climate based Penman, Priestley and Taylor and Stephens and Stewart models.

Table 4. Summary of models statistical performances during the testing period

Model	RMSE (mm/d)	MBE (mm/d)	R^2
Penman	1.87	-1.61	0.75
Priestley-Taylor	1.7	-1.39	0.9
Stephens and Stewart	1.59	-1.25	0.96
ANN-1	0.3	-0.23	0.99
ANN-2	0.8	-0.36	0.98
ANN-3	0.4	-0.25	0.99

The *RMSE*, *MBE* and R^2 statistics for each ANN model during the test period are given in Table 4. The table indicates that the ANN-1 model whose inputs are the air temperature, wind speed, humidity and solar radiation has the smallest *RMSE* (0.3 *mm/d*), absolute *MBE* (0.23 *mm/d*) and the highest R^2 (0.99). Therefore, it is important to take into account the combined influence of all of the meteorological parameter on evaporation. As seen from Table 4, using the air temperature, wind speed, and humidity inputs ANN-2 model resulted in poor estimates when compared with other ANN models. The ANN-3 and Stephens and Stewart models are rather simple and consider only air temperature and solar radiation data. Compared with Stephens and Stewart model, the ANN-3 model performed better from the *RMSE*, absolute *MBE* and R^2 viewpoints. However, the ANN-3 model resulted in lower *RMSE* (0.4 *mm/d*), absolute MBE (0.25 *mm/d*) and higher R^2 (0.99) (Table 4) than the Stephens and Stewart model.

Comparison between the climate based models in this study indicated that the Stephens and Stewart model resulted in the least errors in its prediction with *RMSE* of 1.59, absolute *MBE* of 1.25 and R^2 of 0.96 (Table 4). This was found to be in agreement with the findings of Al-Shalan and Salih [44] who evaluated 23 well-known climatic models of evaporation estimation and concluded that the Stephens and Stewart model was found to perform the best of all ([45,46]). The Priestly and Taylor model followed in model performance with respect to *RMSE*, *MBE* and R^2 values while the Penman model followed in that order (Table 4).

In order to examine the performance of the climate based and ANN models, their estimation results are plotted versus the observed evaporation in the form of scatter plots (Figs. 3 to 8).

The scatter diagrams indicate that the model comparison plots are around 45º straight lines, thus implying that there was no bias effects in the selected models in this paper. This obviously confirms that the prediction obtained from ANN models is more reasonable than the climate based models.

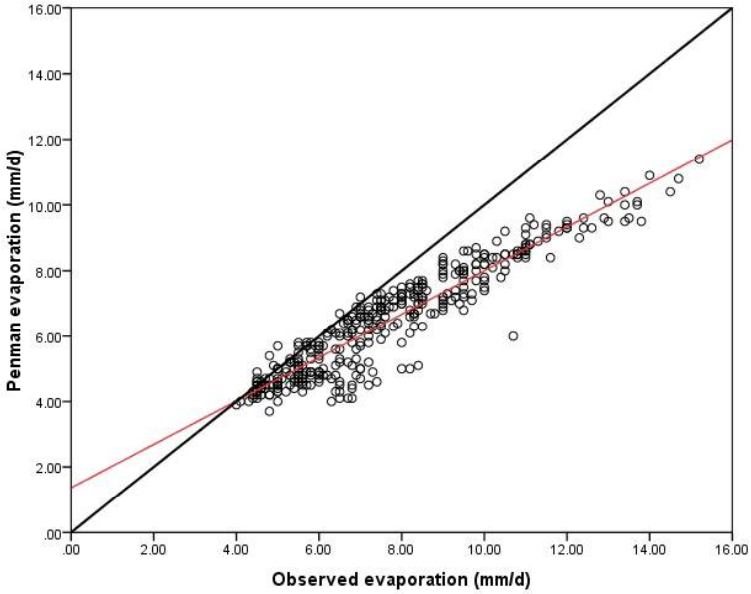

Fig. 3. Scatter plot between observed and predicted values of evaporation during the test period.

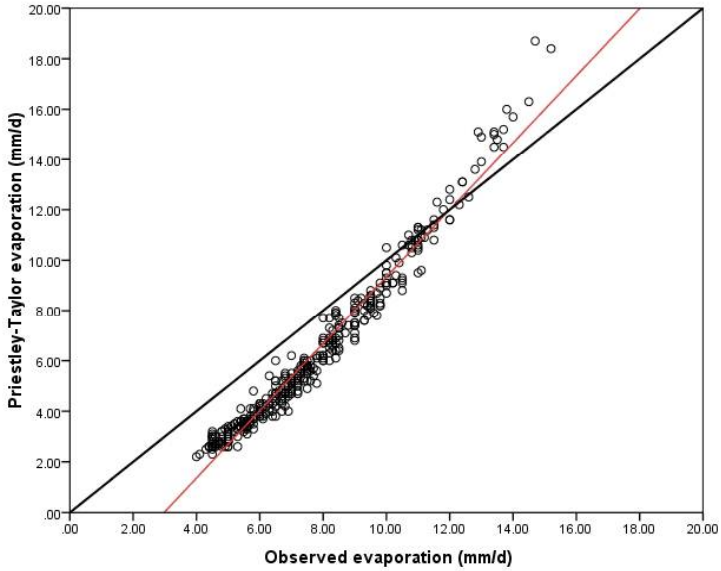

Fig. 4. Scatter plot between observed and predicted values of evaporation during the test period.

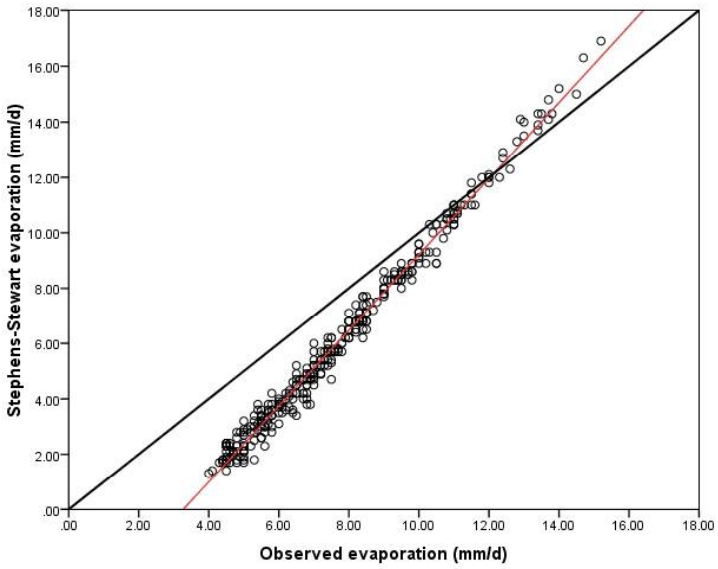

Fig. 5. Scatter plot between observed and predicted values of evaporation during the test period.

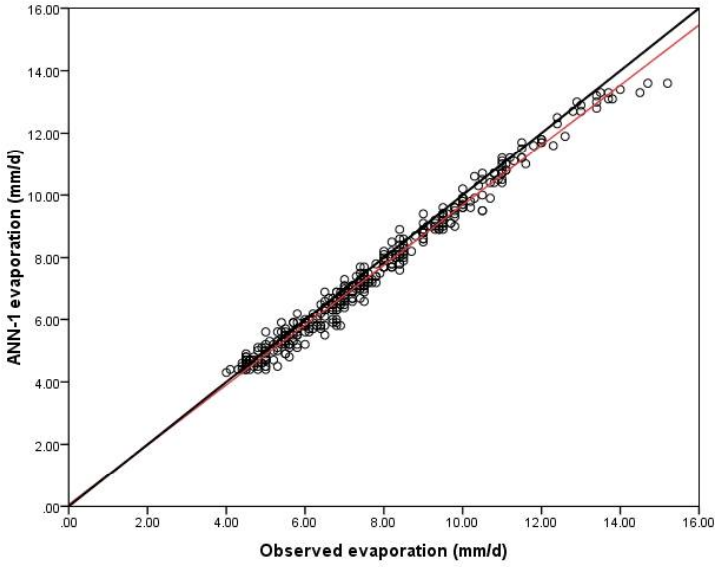

Fig. 6. Scatter plot between observed and predicted values of evaporation during the test period.

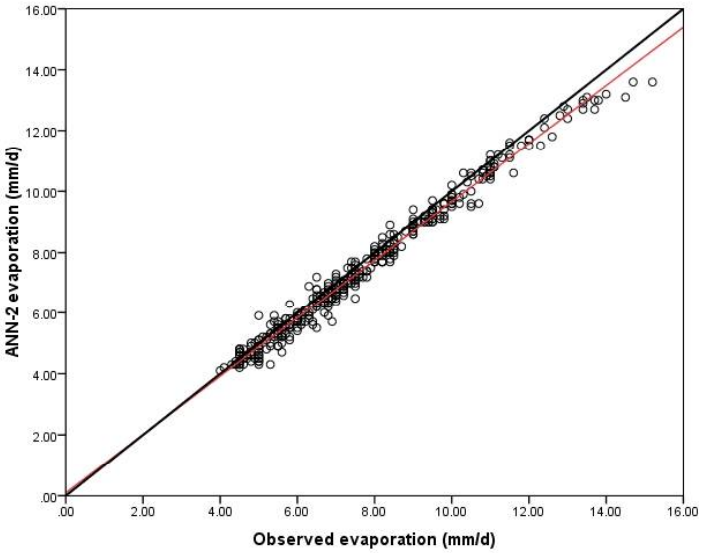

Fig. 7. Scatter plot between observed and predicted values of evaporation during the test period

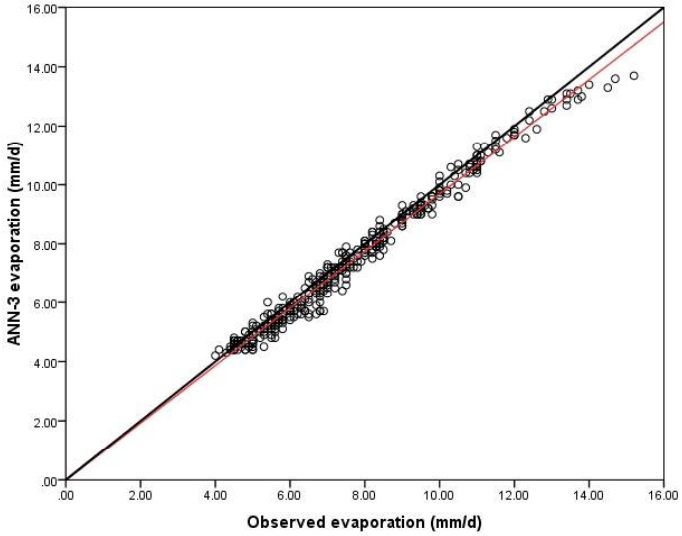

Fig. 8. Scatter plot between observed and predicted values of evaporation during the test period.

To confirm overall performance of the tested models, observed and predicted evaporation values were plotted together for the Penman, Priestly and Taylor, Stephens and Stewart, ANN-1, ANN-2 and ANN-3 models with observed evaporation. Figs. 9 to 14 show the observed evaporation and predictions of the Penman model, Priestly and Taylor model, Stephens and Stewart model, ANN-1 model, ANN-2 model and ANN-3 model respectively.

Figs. 9 to 14 show that all models underestimated evaporation from the Algardibyia Reservoir and their negative values of *MBE* (Table 4) support this observation. Figs. 12, 13 and 14 show that the ANN models (using one year's testing data) resulted in the same trend compared with the observed evaporation data. From the recorded data it was found that the total evaporation for the testing period was 3834 mm while, the estimated evaporation from other models were 2379 mm, 2325 mm, 2246 mm, 2750 mm, 2746 mm and 2744 mm for the Penman, Priestly and Taylor, Stephens and Stewart, ANN-1, ANN-2 and ANN-3 models, respectively. This shows that the ANN models were in agreement with the evaporation record from Algardabiya reservoir. The differences between the observed evaporation and the ANN models are 3% (ANN-1 model), 3.1% (ANN-2 model) and 3.2% (ANN-3 model) in testing period (2006).

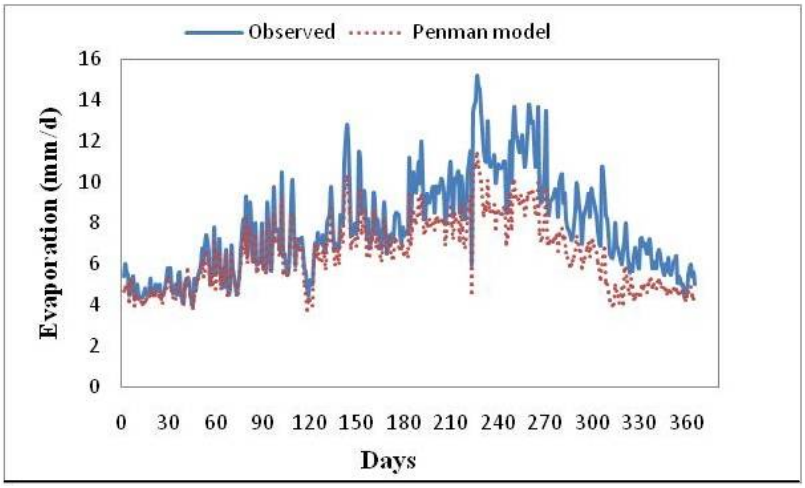

Fig. 9. Evolution of daily evaporation values, observed and predicted by the Penman model during the test period for Algardabiya Reservoir.

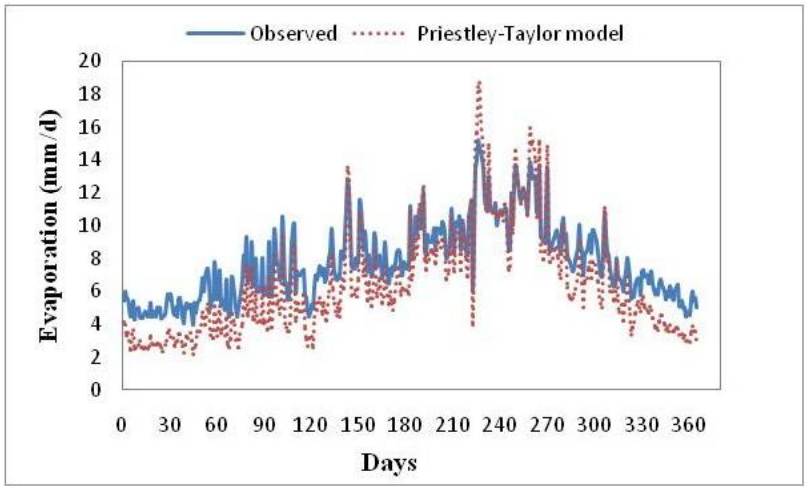

Fig. 10. Evolution of daily evaporation values, observed and predicted by the Priestley-Taylor model during the test period for Algardabiya Reservoir.

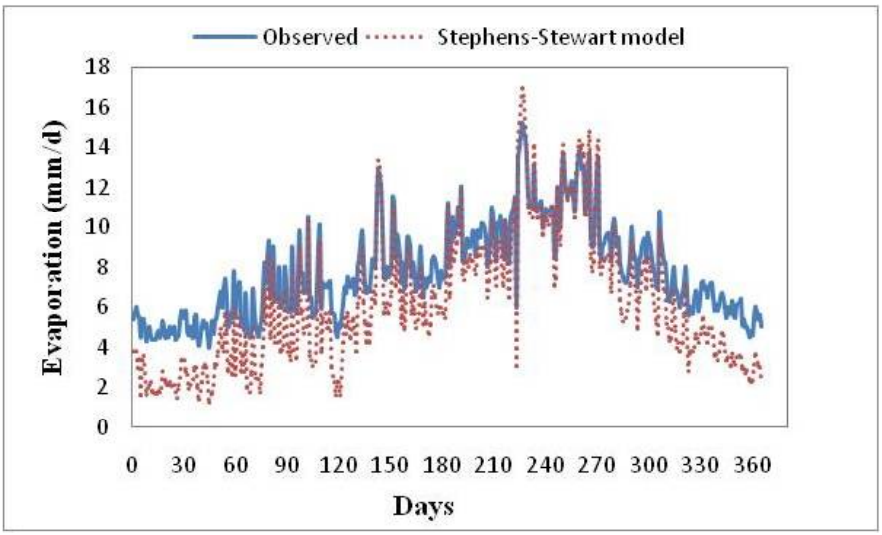

Fig. 11. Evolution of daily evaporation values, observed and predicted by the Stephens-Stewart model during the test period for Algardabiya Reservoir.

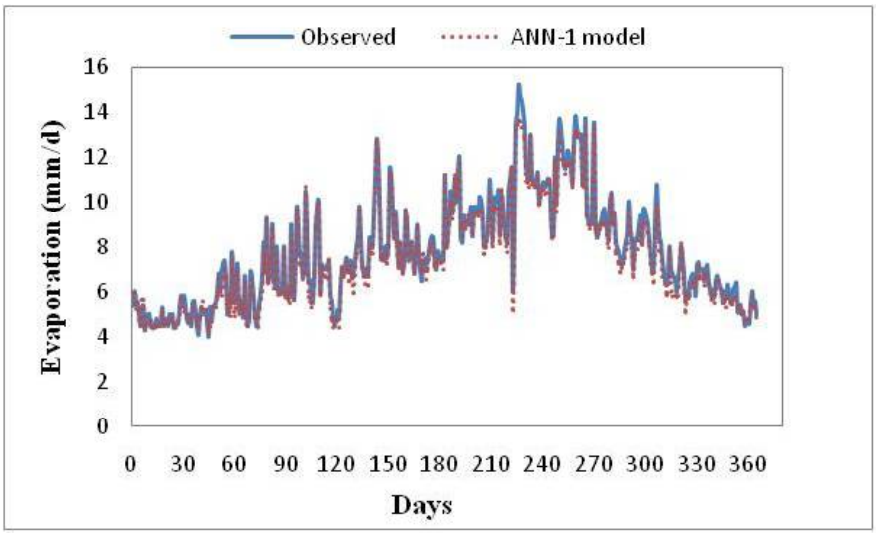

Fig. 12. Evolution of daily evaporation values, observed and predicted by the ANN-1 during the test period for Algardabiya Reservoir.

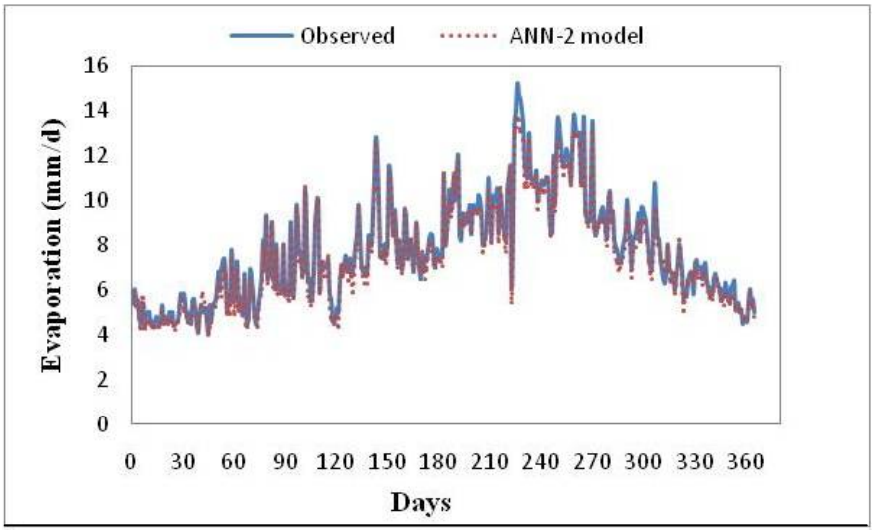

Fig. 13. Evolution of daily evaporation values, observed and predicted by the ANN-2 model during the test period for Algardabiya Reservoir.

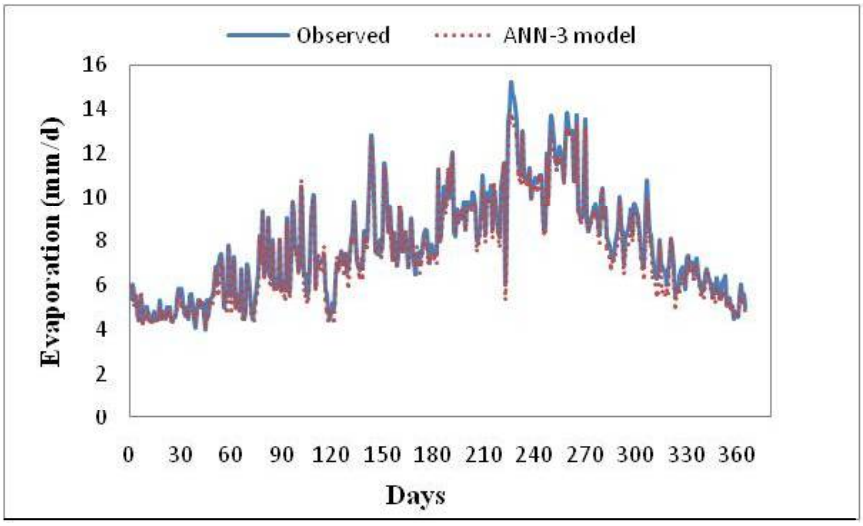

Fig. 14. Evolution of daily evaporation values, observed and predicted by the ANN-3 model during the test period for Algardabiya Reservoir.

4. CONCLUSION

The comparison between Artificial Neural Network and climate based models for estimation of evaporation using climatic variables has been illustrated in this paper. The study demonstrated the accuracy of the Artificial Neural Network technique (ANN) for evaporation modeling compared with climate based models using the Algardabiya Reservoir as a test case. Comparisons were made between the ANN models with climate based Penman, Priestley and Taylor and Stephens and Stewart models. Various statistical measures

(*RMSE*, *MBE*, and R^2) were used to evaluate the performance of the models. Based on the results, the ANN-1 model which had the inputs of air temperature, wind speed, humidity and solar radiation performed the best among all of the models with *RMSE* of 0.3 *mm/d* and absolute *MBE* of 0.23 *mm/d.* This indicates that all of the above variables are needed for better evaporation modeling. However, in some areas, the available data may be the air temperature, T and solar radiation, R_s so, ANN-3 model and Stephens and Stewart model (containing only two inputs, T and R_s) can be used to estimate the evaporation. Among the climate based models evaluated during this study, the Stephens and Stewart performed best with *RMSE* of 1.59 *mm/d* and absolute *MBE* of 1.25 *mm/d* using the test data set. The evaporation could be estimated from easily available data using the ANN approach. The ANN models can be implemented as a module for estimating evaporation data in hydrological modeling studies. Therefore, ANN models can be effectively incorporated in the water management of the reservoir.

COMPETING INTERESTS

Authors have declared that no competing interests exist.

REFERENCES

1. Wang YM, Traore S, Kerh T, Applying evapotranspiration reference model and rainfall contribution index for agricultural water management plan in Burkina Faso. African Journal of Agricultural Research. 2009;4(12):1493-1504.
2. Loucks DP. The Great Manmade River in Libya: Does it Make Sense? in The Third Annual D. R. F. Harleman Honorary Lecture in Environmental Fluid Mechanics. The Department of Civil and Environmental Engineering. The Pennsylvania State University; 2004.
3. Craig I, et al. Controlling Evaporation Loss from Water Storages. National Centre for Engineering in Agriculture Publication. USQ, Toowoomba, Australia; 2005.
4. WMO, Case book on operational assessment of areal evaporation. Secretariat of the World Meteorological Organization. Geneva, Switzerland. ISBN: 9263106355. 194. 1985.
5. Linsley RK, Kohler MA, Paulhus JLH, Hydrology for Engineers. 3rd ed. 1982, New York: McGraw-Hill.
6. Mays LW, Water Resources Handbook. McGraw-Hill, New York. ISBN: 0070411506; 1996.
7. Meyer SJ, Hubard KG, Wilhite DA, Estimating potential evapotranspiration: the effect of random and systematic errors. Agric. For. Meteorol. 1989;46:285-296.
8. Molina Martı´nez, JM, et al., A simulation model for predicting hourly pan evaporation from meteorological data. J. Hydrology. 2006;318:250-261.
9. Webb EK. A pan-lake evaporation relationship. J. Hydrology. 1966;4(1):1-11.
10. Kohler MA, Nordenson TJ, Fox WE, Evaporation from Pans and Lakes. U.S. Dept. Commerce, Weather Bureau Research Paper 38. 1955.
11. Shuttleworth WJ, Macrohydrology - The new Challenge for Process Hydrology. J. Hydrology. 1988;100:31-56.
12. Anderson RE, Energy-budget studies, in water-loss investigations - Lake Hefiier studies. Technical report: U.S. Geol. Survey Prof Paper. 1954;269:71-119.
13. Harbeck GEJ. A practical field technique for measuring reservoir evaporation utilizing mass-transfer theory. U.S. Geol. Surv. 1962;272(E):101-105.

14. Penman HL. Natural evaporation from open water, bare soil and grass. Proc. Roy. Soc. London. 1948;193:120-146.
15. Wang Y, et al. Seasonal temperature-based models for reference evapotranspiration estimation under semi-arid condition of Malawi African Journal of Agricultural Research. 2009;4(9):878-886.
16. Sarangi A, et al. Subsurface drainage performance study using SALTMOD and ANN models. Agric. Water Manage. 2006;84:240-248.
17. Ahmed JA, Sarma AK. Artificial neural network model for synthetic stream flow generation. Res. Water Manage. 2009;21:1015-1029.
18. Han DT, Kwong Li S. Uncertainties in real-time flood forecasting with neural networks. Hydrolog.Process. 2007;21:223-228.
19. Singh M, Datta B. Artificial neural net work modeling for identification of unknown pollution sources in ground water with partially missing concentration observation data. Water Res. Manage. 2007;21:557-572.
20. Hsu K, Gupta HV, Sorooshian S, Artificial neural network modeling of the rainfall-runoff process. Water Resour. Res. 1995;31(10):59-169.
21. Imrie CE, Durucan S, Korre A. River flow prediction using neural networks: Generalization beyond the calibration range. J. Hydrol. Eng. 2000;233(3-4):138-154.
22. McKenzie HS, Elsaleh BO. The Libyan Great Man Made River Project, project overview, Proc. Instn Civ Engr. Wat. Marit and Energy. Proceedings of the ICE - Water Maritime and Energy. 1994;106(2):03-122.
23. GMR, Great Man-made River Water Supply Project, Libya. SPG Media Limited a subsidiary of SPG Media Group PLC; 2006.
24. Fausset LV, Fundamentals of Neural Networks: Architectures, Algorithms and Applications. Upper Saddle River, NJ: Prentice Hall; 1994.
25. Rumelhart DE, Hinton GE, Williams RJ. Learning internal representations by error propagation. In Parallel Distributed Processing: Explorations in the Microstructures of Cognition, eds. Rumelhart, D. E. and McClelland, J. L. MIT Press, Cambridge, MA. 1986;1:318-362.
26. Zhang B, Govindaraju R. Geomorphology-based artificial neural networks (GANNs) for estimation of direct runoff over watersheds. J. Hydrology. 2003;273:18-34.
27. Shirsath PB, Singh AK. A comparative study of daily pan evaporation estimation using ANN, Regression and Climate Based Models. Water Resour Manage. 2010;24:1571-1581.
28. Penman HL. Vegetation and hydrology. Technical Committee No. 53, Common wealth Bureau of Soils, Harpenden, U.K; 1963.
29. Dalton J. Meteorological observations. Mem. Manchester. Lit. Phil. Soc. 1802;5:346-372.
30. Brutsaert WH. Evaporation into the atmosphere: Theory, History and Applications. Reidel, Dordrecht, Holland. 299p. ISBN: 9027712476. 1982;299.
31. Gilman K. Hydrology and Wetland Conservation. New York, USA: John Wiley; 1994.
32. Allen RG, et al. Crop Evapotranspiration: Guidelines for Computing Crop Water Requirements. Irrigation and Drainage Paper 56, FAO, Rome; 1998.
33. Linacre ET. Data-Sparse Estimation of Lake Evaporation, Using a Simplified Penman Equation. Agricultural and Forest Meteorology, 1993; 64:237-256.
34. Shuttleworth WJ, In: Maidment D.R. (Ed.),Evaporation. McGraw-Hill, New York. 1993;4,1–4.53 (Chapter 4).
35. Linacre ET. A simple formula for estimating evaporation rates in various climates, using temperature data alone. Agric. Meteorol. 1977;18:409-424.
36. Priestley CHB, Taylor RJ. On the assessment of the surface heat flux and evaporation using large-scale parameters. Mon. Water Rev. 1972;100:81-92.

37. Stewart RB, Ruose WR. A simple method for determining the evaporation from shallow lakes and ponds. Water Resour. Res. 1976;12:623-628.
38. Stewart RB, Ruose WR. Substantiation of the Priestley-Taylor parameter ALPH = 1.26 for potential evaporation in high latitudes. J. Appl. Meteorology. 1977;16:649-650.
39. De Bruin HAR, Keijman JQ. The Priestley-Taylor evaporation model applied to a large, shallow lake in the Netherlands. J Applied Meteorology. 1979;18:898-903.
40. Stephens JC. Stewart EH. A comparison of procedures for computing evaporation and evapotranspiration. Publication 62, International Association of Scientific Hydrology. International Union of Geodynamics and Geophysics, Berkeley. 1963;123–133.
41. Fox DG. Judging air quality model performance. Bull. Amer. Meteorol. Soc. 1981;62:599-609.
42. Willmott CJ. Some comments on the evaluation of model performance. Bull. Amer. Meteorlo. Soc. 1982;63:1309-1313.
43. Kennedy JB, Neville AM. Basic Statistical Methods for Engineers and Scientists. 3rd ed. Harper and Row, New York; 1986.
44. Al-Shalan A, Salih A. Evapotranspiration estimation in extremely arid areas. ASCE Journal of Irrigation and Drainage Engineering. 1987;113: 565-574.
45. Sudheer KP, et al. Modelling evaporation using an artificial neural network algorithm. J. Hydrol. Process. 2002;16:3189-3202.
46. Kisi O. Daily pan evaporation modelling using a neuro-fuzzy computing technique. J. Hydrology. 2006;329:636- 646.

Peer-review history:
The peer review history for this paper can be accessed here:
http://www.sciencedomain.org/review-history.php?iid=580&id=5&aid=5126